On the limit of superhydrophobicity: defining the minimum amount of TiO_2 nanoparticle coating

Janne Haapanen[1], Mikko Aromaa[1], Hannu Teisala[2,3], Paxton Juuti[1], Mikko Tuominen[2,4], Markus Sillanpää[5], Milena Stepien[6,7], Jarkko J. Saarinen[6], Martti Toivakka[6], Jurkka Kuusipalo[2] and Jyrki M. Mäkelä[1]

[1] Aerosol Physics, Laboratory of Physics, Faculty of Natural Sciences, Tampere University of Technology, Tampere, Finland

[2] Packaging Technology Research Team, Laboratory of Materials Science, Tampere University of Technology, Tampere, Finland

[3] Department of Physics at Interfaces, Max Planck Institute for Polymer Research, Mainz, Germany

[4] Bioscience and Materials / Surface, Process and Formulation, RISE Research Institutes of Sweden, Stockholm, Sweden

[5] Laboratory Centre, Finnish Environment Institute, Helsinki, Finland

[6] Laboratory for Paper Coating and Converting, Abo Akademi University, Turku, Finland

[7] Academic Centre for Materials and Nanotechnology, AGH University of Science and Technology, Krakow, Poland

Keywords: nanoparticles; nanocoatings; Liquid Flame Spray; wetting; superhydrophobic; titanium dioxide, TiO_2

ABSTRACT

Fabrication of superhydrophobic surfaces in large scale has been in high interest for several years, also titanium oxide nanostructures having been applied for the purpose. Optimizing the amount and structure of the TiO_2 material in the coating will play a key role when considering upscaling. Here, we take a look at fabricating the superhydrophobic surface in a one-step roll-to-roll pilot scale process by depositing TiO_2 nanoparticles from a Liquid Flame Spray onto a moving paperboard substrate. In order to find the minimum amount of nanomaterial still sufficient for creating superhydrophobicity, we varied nanoparticle production rate, flame distance from the substrate and line speed. Since the deposited amount of material sideways from the flame path was seen to decrease gradually, spatial analysis enabled us to consistently determine the minimum amount of TiO_2 nanoparticles on the substrate needed to achieve superhydrophobicity. Amount as low as 20-30 mg/m^2 of TiO_2 nanoparticles was observed to be sufficient. The scanning electron microscopy revealed that at this amount, the surface was covered with nanoparticles only partially, but still sufficiently to create a hierarchical structure to affect wetting significantly. Based on XPS analysis, it became apparent that TiO_2 gathers hydrocarbons on the surface to develop the surface chemistry towards hydrophobic, but below the critical amount of TiO_2 nanoparticles, the chemistry could not enable superhydrophobicity anymore. While varying the deposited amount of TiO_2, besides the local spatial variance of the coating amount, also the overall yield was studied. Within the text matrix, a yield up to 44 % was achieved. In conclusion, superhydrophobicity was achieved at all tested line speeds (50 to 300 m/min), even if the amount of TiO_2 varied significantly (20 to 230 mg/m^2).

1. INTRODUCTION

Generation of superhydrophobic surfaces has been of high interest to both scientific and industrial fields. There are various methods for manufacturing superhydrophobic surfaces, such as laser etching [1], photocatalytic lithography [2], wet-chemical route [3,4], electrochemical deposition [5,6], electrospinning [7], chemical vapor deposition (CVD) [8] and sol-gel method [9]. Using nanoparticles in surface functionalization has several advantages: e.g. high purity, wide range of coating materials and that amount of material is extremely low compared to macroscopic surface treatment methods. Usually high-speed fabrication of functional coatings refers to a roll-to-roll coating process, where a substrate unwinds from one roll and winds to another. In this process, a coating is applied in one or several steps on the substrate between the two rolls. When discussing about roll-to-roll nanocoating processes, line speeds in most cases are in the range of a meter to few meters per minute [10-14]. It is a big advantage if coating is performed in one-step process with high nanoparticle production rate, which requires only a simple modification to the roll-to-roll process and enables faster line speeds. Finding the minimum amount of TiO_2 needed for superhydrophobicity is in the key role for future development and aiming for more efficient manufacturing of superhydrophobic surfaces.

Gas-phase synthesis methods for nanoparticle production are widely used in industrial and scientific fields, and especially flame based methods are considered to be optimal for up-scaling [15-17]. Produced nanoparticles can either be collected as powder and subsequently applied on surfaces by various methods [18] or deposited directly onto surfaces forming functional nanocoatings [19,20]. Similarly to other flame synthesis methods [21,22], Liquid Flame Spray (LFS) method has also been widely used in nanoparticle generation [23]. Recently, LFS has been used for manufacturing functional nanocoatings in a roll-to-roll process [24-27]. These nanocoated paperboard surfaces can be used e.g. in micro fluidics [28] or as

anti-microbial surfaces [29]. In previous studies, roll-to-roll line speed of 50 m/min has been used for producing superhydrophobic and superhydrophilic surfaces [24,25,30,31]. To our knowledge, higher line speeds than 150 m/min have not been reported before. Higher line speed can be used to minimize coating amount without changing other process parameters. We used pilot scale paper converting machine with line speeds of 50, 100, 200 and 300 m/min aiming for superhydrophobic surfaces, with minimal amount of nanocoating on the surface. Especially for industrial scale applications, there is a demand for high line speeds. Commercially available pigment coated paperboard (200 g/m^2) was chosen as the substrate to be able to compare the results to previous studies with lower line speeds. It has been shown that LFS-generated TiO_2 nanoparticles produce superhydrophobic surfaces with line speed of 50 m/min, but the effect of higher line speeds to nanocoating behavior need to be analyzed more closely. With the line speed of 50 m/min, paperboard surface is covered with excess amount of nanoparticles, therefore our aim is to achieve a superhydrophobic surface with a lower amount of nanoparticles and find out what is the minimum amount of TiO_2 needed for superhydrophobicity. Here the TiO_2 nanoparticles produced with the LFS consists mainly of anatase, with a small fraction of rutile [30]. Different LFS process parameters were used in the paperboard coating and they were also optimized to achieve superhydrophobicity with an adequate process yield. Here the yield is defined as the share of produced nanoparticles that adhere on the paperboard.

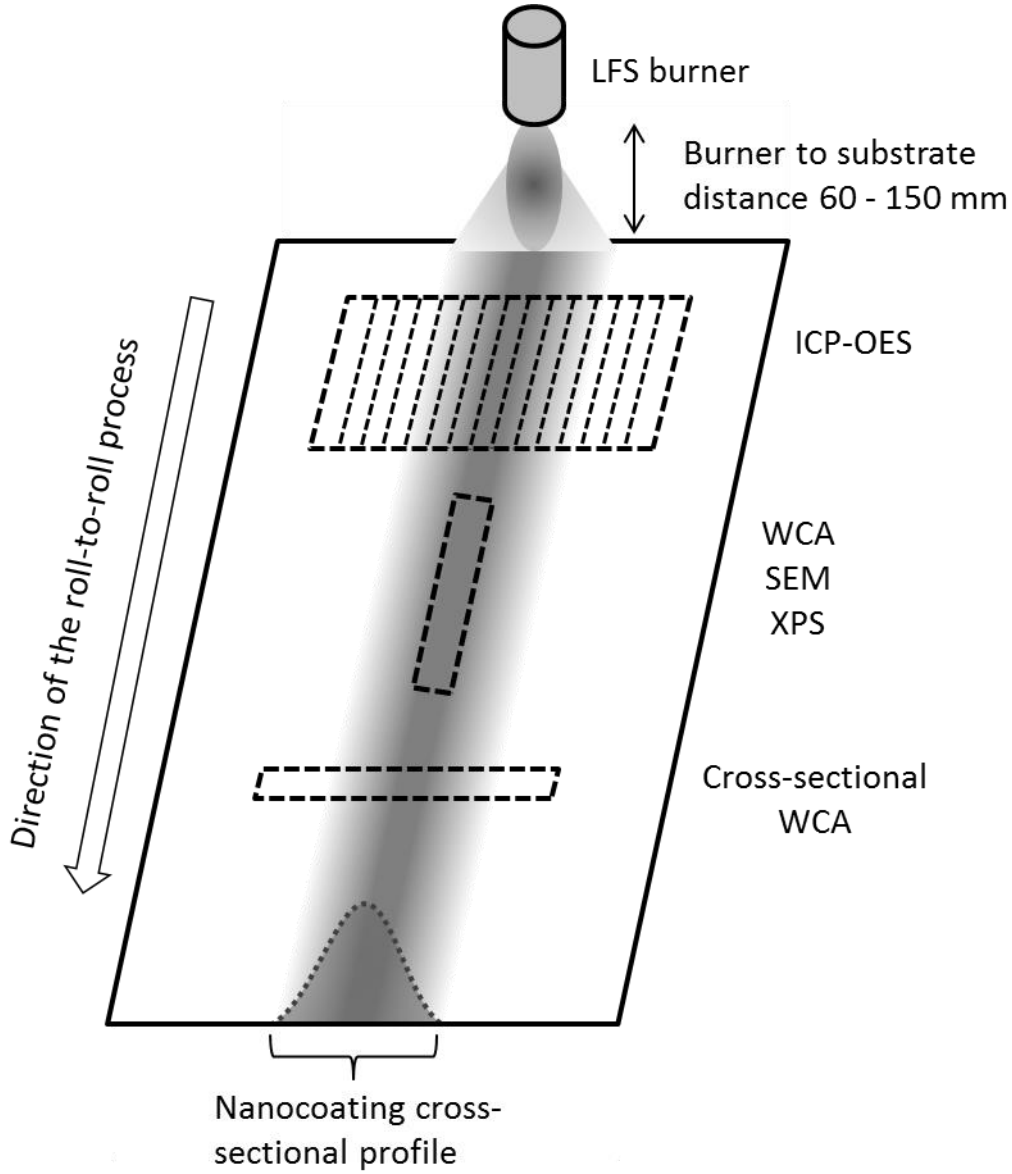

Figure 1: Schematic graph of how the different analyses were made on the nanocoated paperboard.

Table 1. Five process parameters of LFS1 and LFS2 applied in this study.

	Precursor concentration (Ti mg/ml)	Precursor feed rate (ml/min)	Burner to substrate distance (mm)	Production rate of TiO_2 (mg/min)	Line speeds (m/min)
LFS1	50.0	32.0	150	2670	50, 100, 150
LFS2	50.0	11.6	60	968	50, 100, 200, 300

2 EXPERIMENTAL SECTION

2.1 Liquid Flame Spray for nanoparticle production

Liquid Flame Spray (LFS) is a versatile aerosol synthesis method for nanoparticle production. In LFS method, liquid precursor solution is injected into a turbulent hydrogen-oxygen flame. Precursor evaporates in the hot flame and due to subsequent rapid cooling, precursor containing gas becomes supersaturated, which leads to nucleation. The aerosol processes of the LFS method have been described in more detail previously [27,30,32]. By adjusting the process parameters, such as the precursor concentration and feed rate, and the flow rates of the burner gases, properties of the produced nanoparticle aerosol can be tuned. With high production rates, nanoparticles form agglomerates, consisting of multiple primary nanoparticles. Originally, LFS was developed for coloring art glass by nanoparticles [33]. In past years, LFS has been used more and more to fabricate functional nanocoatings for various substrates [25,34-37], but also as a tool for test aerosol production [38] and to create optimal surface structure for superamphiphobic surface treatments [39,40]. In this study, Titanium(IV)-isopropoxide (TTIP, Alfa Aesar 98%+) was pre-mixed with 2-propanol (VWR, HiPerSolv CHROMANORM, HPLC grade) resulting metallic Ti-concentration of 50.0 mg/ml in liquid precursor solution. Two different LFS coating parameters were used for paperboard coating: LFS1 and LFS2. Precursor feed rate was fixed at 32.0 ml/min for LFS1 and 11.6 ml/min for LFS2, resulting in TiO_2 production rates of 2670 and 968 mg/min, respectively. Gas flow rates for H_2 and O_2 in all experiments were fixed at 50 l/min and 15 l/min, respectively. Process parameters are summarized in Table 1. All of the LFS-generated nanocoatings were applied on commercially available pigment coated paperboard (200 g/m^2) in a pilot scale roll-to-roll paper converting machine, located at Tampere University of Technology. Both LFS1 [27,41,42] and LFS2

[24,25,30,43,44] parameters have been previously used in several publications in nanocoatings for paper and paperboard.

2.2. Spatial distribution of deposited mass

The deposited line of nanoparticles from single pass of the LFS flame nozzle is limited in width due to the evident finite size of the flame itself. Based on a visual inspection of the deposited line for darker nanoparticle material than TiO_2, such as Ag or Fe_xO_y, it is expected that the flame generates a deposited line of nanoparticles with higher concentration in the middle, which decreases towards the edges. A feasible assumption is that this deposited mass distribution follows spatially a normal distribution. The spatial distribution also arises from the fact that the cross section of the flame is round, and also from having slightly hotter parts in the middle. It evidently produces higher temperature gradient between the flame and substrate in the middle, which in turn, furthermore, causes higher deposition velocity of the particles and thus higher concentrations of deposited mass in the center part of the line (Figure 2b). We approached this phenomenon as follows: we measure certain properties of the coating in the center of the deposited line, and later we continue performing the analyses at different points towards the edges of the pattern. Additionally, a total amount of the integrated cross section of the deposited mass can be analyzed.

2.3 Water contact angle measurement

Water contact angles (WCA) were determined using KSV CAM 200 Optical Contact Angle Meter (KSV Instruments Oy, Helsinki, Finland). The treated samples were stored and the measurements were performed in controlled atmosphere (50 ± 2% RH, 23 ± 2 °C). Distilled water (H_2O, surface tension 72.8 mN/m) was used as the probe liquid. Each WCA value is an average of five individual measurements taken from the centerline of a coating (Figure 1). The contact angle value was measured approximately 3 s after the droplet placement to allow the

vibrations of the droplet to settle down, but before evaporation and possible penetration of liquid into the substrate did not dramatically affect the droplet volume or the contact angle. The droplet volume used for contact angle measurements was 5 µl. WCA measurement were carried out in several different time spans: immediately after the coating process and after 1, 2, 7, 30, 90 and 365 days, in order to observe aging effect on the wettability of the nanocoated surface. Also, cross-sectional WCA profile was determined as described in Figure 1, with a total width of 110 mm.

2.4 X-Ray Photoelectron spectroscopy

The degree of oxidation and chemical composition of the treated samples were determined by XPS using a Physical Electronics Quantum 200 ESCA instrument, equipped with a monochromatic Al Kα X-ray source operating at 25 W of power. The pass energy for the survey spectra was 117.4 eV. The charge compensation was carried out with a combination of a low-energy electron flood gun and a low-energy ion source (Ar). The XPS measurements were performed one day and 90 days after the LFS treatments to analyze chemical changes on the surface. Each XPS measurement value is an average of three individual measurements taken from the centerline of a coating (Figure 1). Details of the XPS analysis are described more detailed in previous publications [24,42].

2.5 Field Emission Scanning Electron Microscopy

The surfaces were imaged with ultra-high resolution field emission gun scanning electron microscope (FE-SEM, Zeiss ULTRAplus). Due to the resistive nature of paperboard and TiO_2 nanoparticles, the samples were sputter coated with a thin carbon film prior to FE-SEM imaging for better conductivity. FE-SEM analysis was performed on the centerline of the nanocoating (Figure 1).

2.6 Inductively Coupled Plasma Optical Emission Spectrometry

For the titanium analysis, the paperboard samples with and without TiO_2 nanoparticle coating were first placed into the quartz test tubes for the extraction. Prior to microwave digestion (Milestone, Italy), 2 ml of nitric acid and 2 ml of sulphuric acid were added. The digestion was operated at 240 °C and 40 bar for 45 minutes. After 15-min cooling, deionized milli-Q water was added until 30 ml total volume was reached. Titanium concentration was determined by using an Inductive Coupled Plasma Optical Emission Spectrometer (ICP-OES; Varian Vista PRO Radial, Australia). For the ICP-OES analysis of LFS2, 30 cm wide cross sectional paperboard strip was analyzed (Figure 1) to define total yield of the process. ICP-OES analysis for LFS1 was carried out from the centerline to confirm the spatial distribution of the LFS nanocoating in a roll-to-roll process.

3 RESULTS AND DISCUSSION

3.1 Titanium analysis

The spatial distribution of the TiO_2 nanocoating was verified by cutting the coated paperboard into 10 mm slices along the coating line and analyzing them by ICP-OES. Results of the ICP-OES is presented in Figure 2 along with measured WCA values. The spatial distribution of the TiO_2 nanocoating shows a dependency between the TiO_2 amount and the wetting behavior. Correlation between the TiO_2 mass on the surface and the WCA is illustrated in more detail in Figure 3. Results show that as low amount as 20 mg/m^2 of TiO_2 nanoparticles is enough to produce superhydrophobic nanocoating with line speeds of 50 and 100 m/min. Excess amount of TiO_2 does not depress wettability and the surface is still superhydrophobic even with high TiO_2 concentrations.

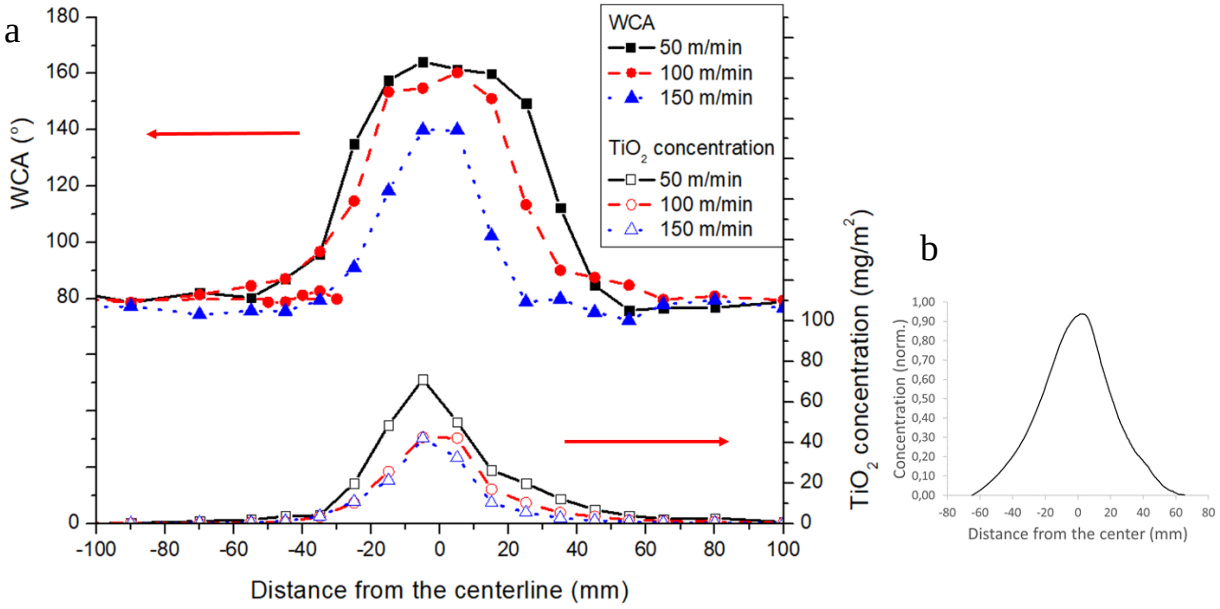

Figure 2: TiO_2 concentration and water contact angles (WCA) of the LFS-treated (LFS1) and reference paperboard samples, determined with ICP-OES (a). Color intensity of the coating measured to confirm the spatial distribution (b).

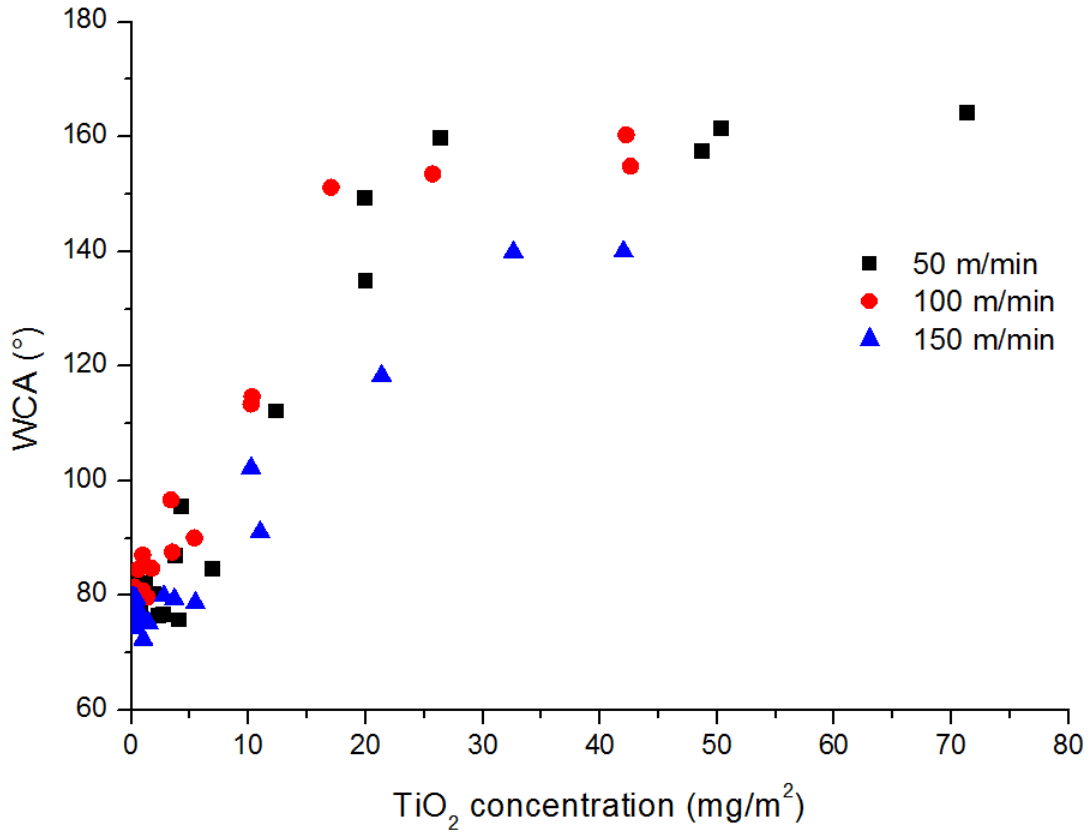

Figure 3: Relation between the amount of TiO_2 on the surface and surface wettability (LFS1).

With the knowledge of the coating parameters LFS1, the improved coating parameters LFS2 were used to carry out roll-to-roll coating with line speeds of 50, 100, 200 and 300 m/min. The aim was to get the superhydrophobic nanocoating with less nanoparticles and with relatively good yield. 30 cm wide pieces of the nanocoated paperboard were analyzed by ICP-OES to obtain the yield of the process. Such a wide sample size was chosen to ensure measuring the total mass of deposited nanoparticles. This information is useful in the future studies when coating is carried out with several burners in a row. Results of the ICP-OES with line speeds of 50, 100, 200 and 300 m/min are presented in Table 2 and in Figure 4. The coated area in Table 2 means the completely analyzed area: most of the coating is distributed into a smaller area. ICP-OES analysis presents results of the total TiO_2 concentration of the analyzed area, thus the coated area is presented as such a large value. Since the substrate material is pigment coated paperboard, the substrate itself contains TiO_2 as a white pigment. Amount of TiO_2 from the substrate is deducted from the results in Table 2. Reference paperboard has TiO_2 concentration of 41.4 mg/m^2. After deduction of the reference concentration from the LFS treated samples, deposited TiO_2 amounts are 23.6 mg/m^2, 9.2 mg/m^2, 7.1 mg/m^2 and 4.1 mg/m^2 for line speeds of 50 m/min, 100 m/min, 200 m/min and 300 m/min, respectively. Total production rate of TiO_2 from the LFS treatment was 968 mg/min with all line speeds. Yield of the process is relatively good with all tested line speeds. Highest yield is achieved with line speed of 200 m/min, as 43.8 % of the produced TiO_2 nanoparticles are deposited on the paperboard surface. This is a significant improvement in the yield compared to previously reported 9-20 % yield with LFS1 parameters with different line speeds [27]. Lower distance between the burner and the substrate is the most important yield improving difference between LFS1 and LFS2, mainly due to increased temperature gradient between the flame and the substrate, which improves thermophoretic deposition efficiency.

Table 2: The amount of TiO_2 from the LFS treatment and the yield of the process with different line speeds (LFS2).

Line speed (m/min)	50	100	200	300
Amount of TiO_2 in the coating (mg/m^2)	23.6	9.2	7.1	4.1
Coated area (m^2/min) from a 30 cm wide sample	15	30	60	90
Yield of the process (%)	36.4	28.4	43.8	38.0

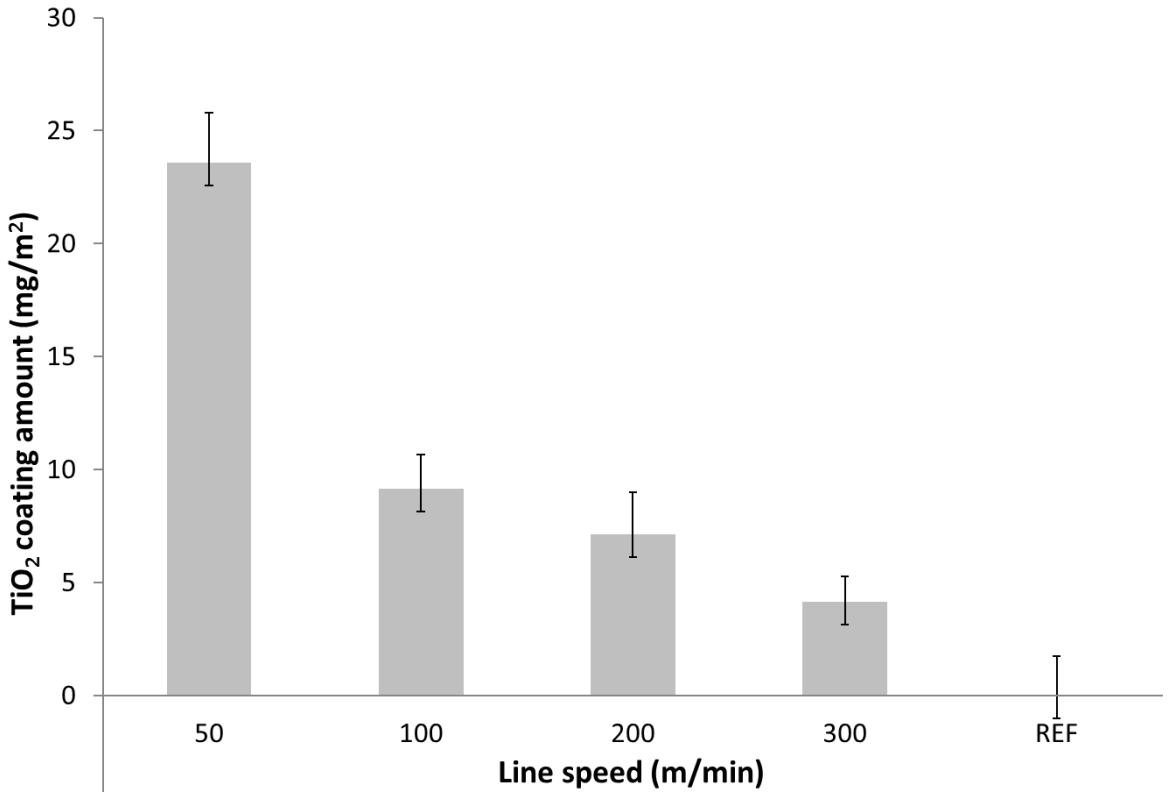

Figure 4: TiO_2 coating amount of the LFS-treated (LFS2), determined with ICP-OES. TiO_2 concentration is defined as an average for a 30 cm wide samples.

3.2 Surface wettability

Wettability of the coating was evaluated by measuring a static water contact angle (WCA) several times after the coating process. WCA measurements were performed immediately after the coating process as well as 1, 2, 7, 30, 90 and 365 days after the coating. The observed wetting behavior undergoes changes over time, as the material ages after the coating. This effect is mostly due to accumulation of carbonaceous matter from air and has been previously reported in several studies [24,45,46].

With all tested line speeds, level of hydrophobicity increases during time, as presented in Figure 5. With a line speed of 50 m/min, the surface is superhydrophobic (WCA > 150 °) immediately after the LFS treatment. With higher line speeds, superhydrophobicity is achieved after one week. WCA values in Figure 2 are determined from the center line of the LFS coating. The WCA value of the reference paperboard remains stable at 78 °.

Superhydrophobicity of the TiO_2-nanocoated paperboard was measured at different time points after the coating process. WCA measurements were carried out immediately after as well as 1, 2, 7, 30, 90 and 180 days after the coating process. The WCA values increase from the initial measurement after the coating and they stabilize in a few days after the coating.

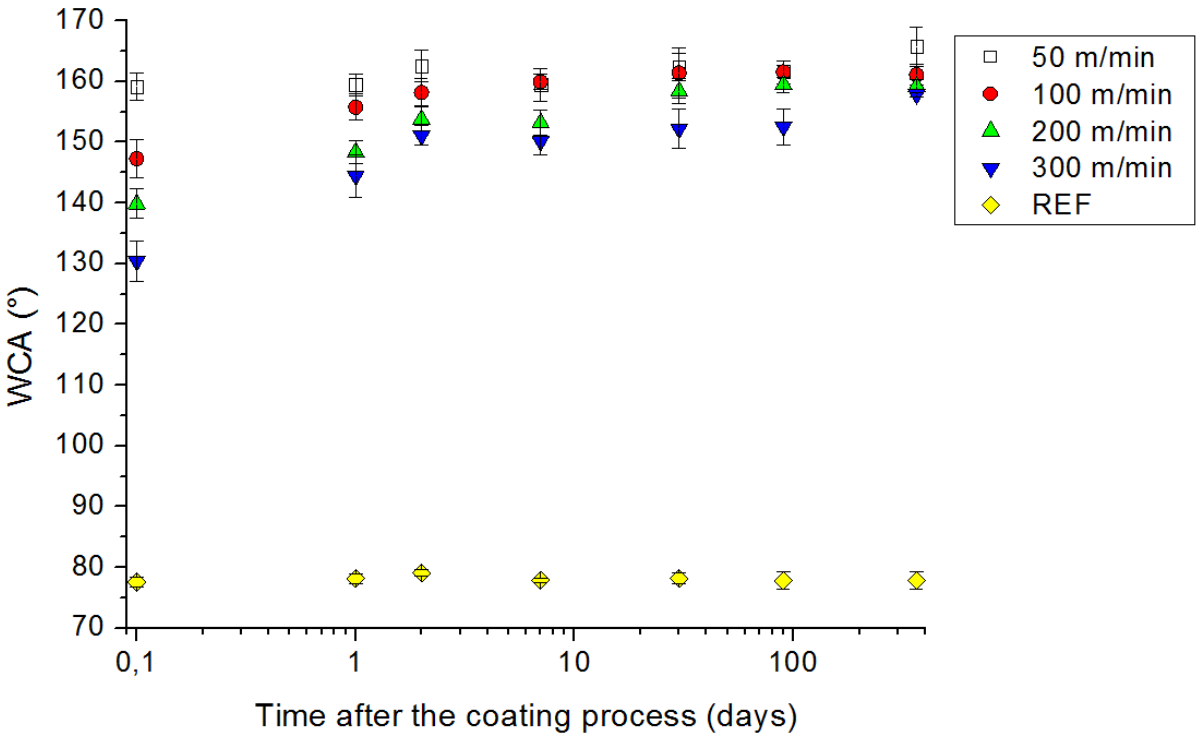

Figure 5: WCA values as a function of the time after the coating process with different line speeds (LFS2).

3.3 Chemical changes on the surface with time

The hydrophobicity of the LFS-treated area of the paperboard surface increases with time. Based on the XPS measurements, this is due to chemical changes on the surface. TiO_2 has a tendency to accumulate carbonaceous matter that builds up on top of the nanoparticles as time goes by. These changes in the chemical composition of the LFS-treated surfaces were analyzed by XPS from the centerline of the nanocoating. In the previous studies, carbon to oxygen ratio (C/O) has shown a strong correlation with wettability [24,42]. In the Figure 6, C/O is presented at different line speeds. The LFS-treated surfaces were analyzed after one day and after 90 days of the coating process. Carbon to oxygen ratio increases in 90 days with all the line speeds, indicating accumulation of carbonaceous compounds on the surface. Similar increase in the

C/O ratio is not observed in reference paperboard. Additionally, the hydrophobicity also increases as C/O ratio increases with time.

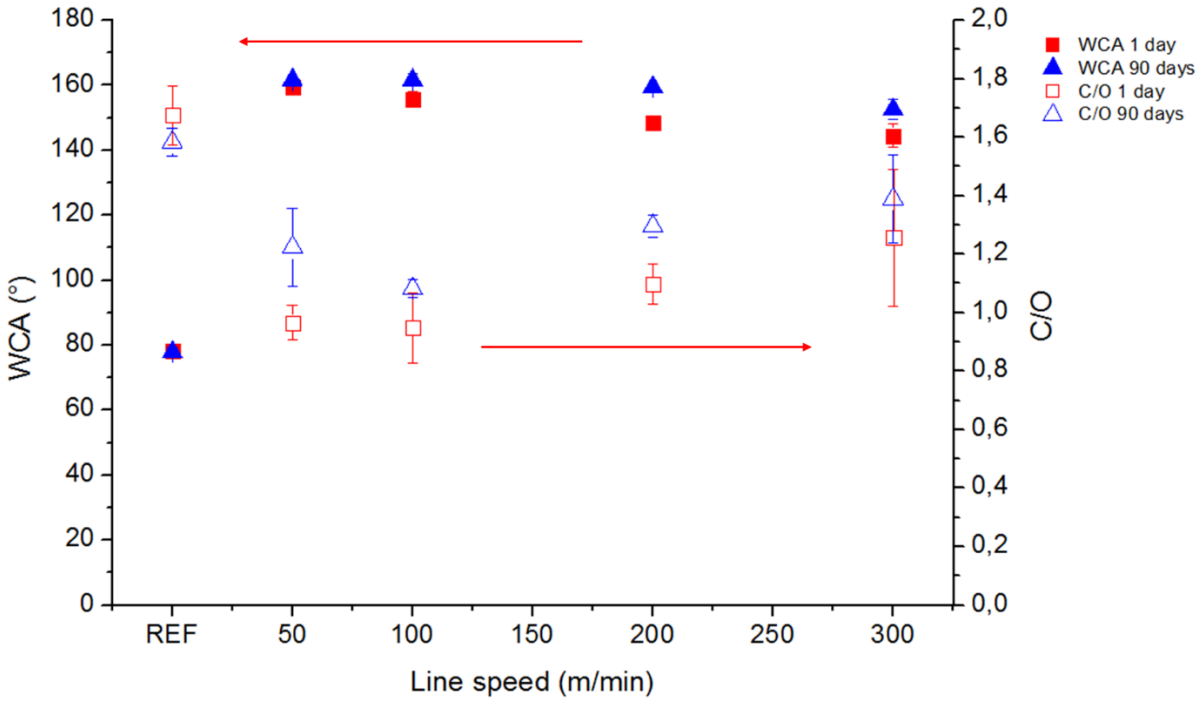

Figure 6: WCA and C/O ratio comparison between 1 day and 90 days after the LFS treatment.

Additionally, the line speed has an effect on the coating width. As is to be expected, coating width gets narrower as the line speed increases. Cross-sectional wetting behavior with different line speeds was analyzed to determine the width of the superhydrophobic area. Cross-sectional WCA values with different line speeds are presented in Figure 7. With line speed of 50 m/min, increased hydrophobicity is achieved in approximately 50 mm and superhydrophobicity in 40 mm cross-sectional area. Width of the superhydrophobic area with line speeds of 100, 200 and 300 m/min are 20, 15 and 10 mm, respectively. Cross-sectional WCA analysis was performed 365 days after the LFS treatment to maximize the difference between the hydrophobic and non-hydrophobic areas.

Information about spatial distribution and the total mass of the coating were used to estimate distribution of the mass in the coating line with LFS2 parameters. Measured cross-sectional

wetting behavior and estimated TiO_2 distribution are presented in Figure 7. Width of the superhydrophobic line gets narrower as the line speed increases. This is an expected phenomenon, as the coating amount decreases and sufficient amount of TiO_2 is not deposited on the edges of the coating line.

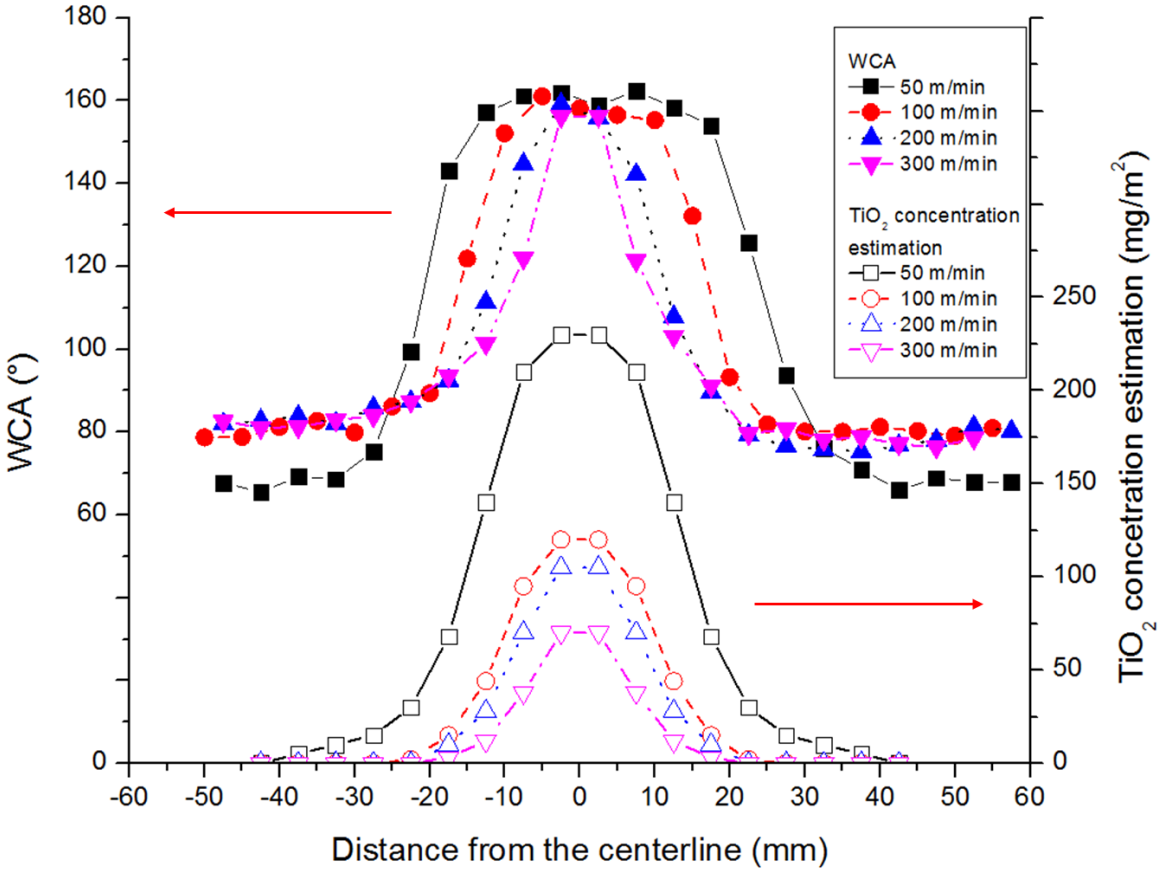

Figure 7: Cross-sectional WCA values with different line speeds and estimation of the TiO_2 concentration, based on the wettability and the total amount of TiO_2 on the surface (LFS2).

3.4 SEM analysis

FE-SEM graphs with two different magnifications are presented in Figure 8. By comparing these graphs with the different line speeds, it is possible to determine the decreasing amount of TiO_2 nanoparticles on top of the paperboard as the line speed increases. With line speeds of 50 and 100 m/min, the surface is fully covered by TiO_2 nanoparticles, but with a line speed of 200

m/min, the paperboard surface is partially visible and with 300 m/min line speed approximately half of the paperboard is visible and the other half is covered by TiO_2 nanoparticles. By comparing these results with the WCA measurements, it is noticeable that the surface is capable of repelling water even if the surface is not fully covered by the TiO_2 nanoparticles and superhydrophobicity was achieved with line speeds of 200 and 300 m/min. In our previous study [43], cross-sectional SEM image of TiO_2 nanocoated paperboard surface was presented with a coating thickness above 500 nm, which gave a strong indication of full coverage of the paperboard surface with a line speed of 50 m/min, and explains why full coverage of the surface was also achieved with the line speed of 100 m/min.

Nanocoatings in Figure 8 consist of agglomerates of TiO_2 nanoparticles with primary particle size of approximately 20-30 nm. The production rate of TiO_2 in the LFS process is sufficiently high (968 mg/min) such that agglomeration cannot be avoided. Some micro-scale roughness is observable on the reference paperboard and with the addition of TiO_2 nanoparticles. The surface has multi-scale roughness, which enables the superhydrophobic behavior. Conceptual side view of the nanocoating in Figure 8 is based on the previous publications about porous nanoparticle coatings [43,47,48].

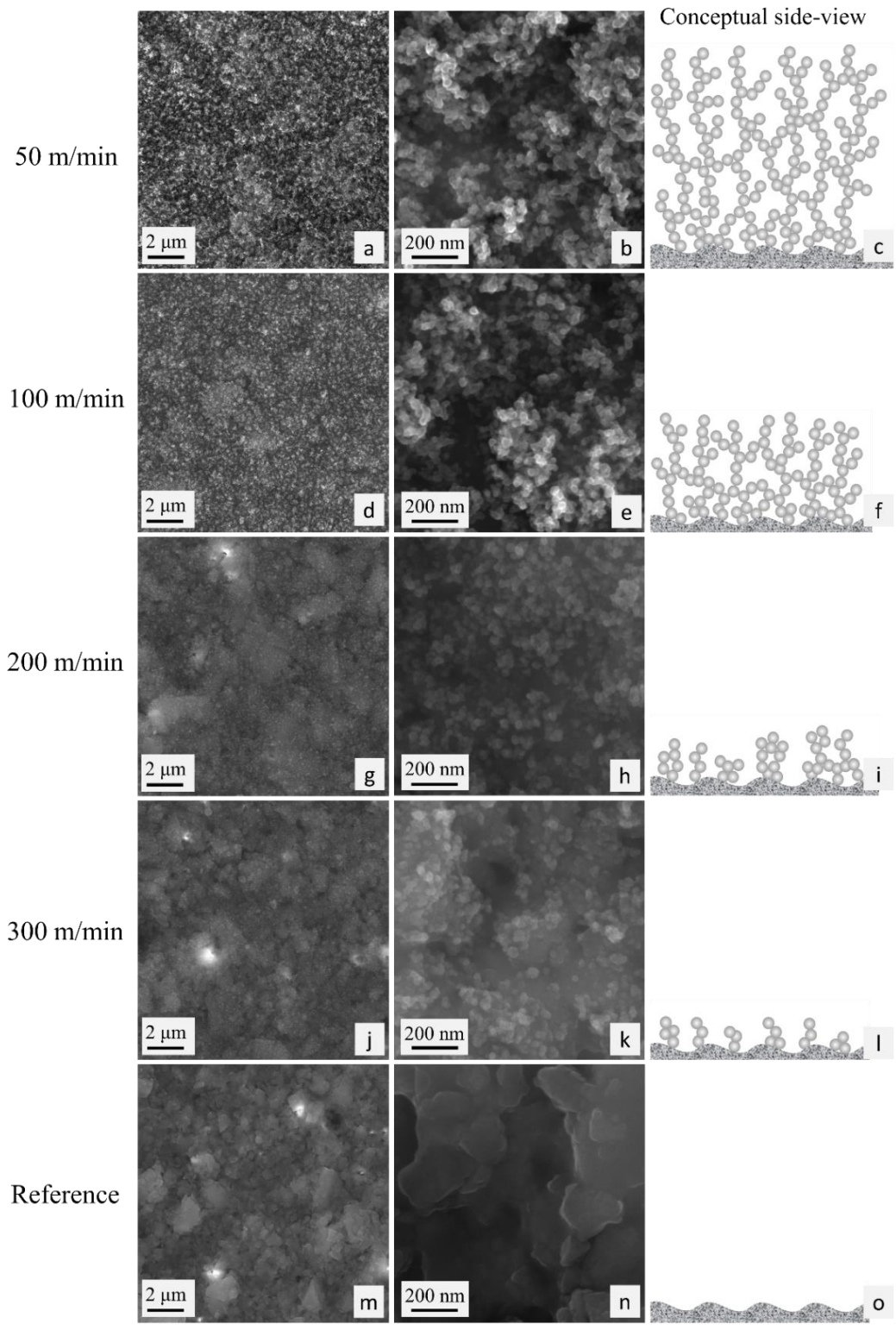

Figure 8: FE-SEM images of the paperboard surfaces coated at various line speeds. The left column (a, d, g, j & m) is with lower magnification (scale bar 2 µm) and the middle column (b, e, h, k & n) with higher magnification (scale bar 200 nm). Conceptual side view is presented in the right column (c, f, i, l & o).

3.5. Interpretation of nanoparticle amount

Based on the ICP-OES data, the minimum TiO_2 concentration on the surface to ensure superhydrophobicity is approximately 20-30 mg/m^2, which is equivalent to approximately 5-6 nm thick solid layer of TiO_2 on the surface. It is apparent that in our case, the layer consisting of minimum amount of nanoparticles is not hermetically solid, but the substrate is actually peeking through. In principle, the experimentally determined minimum amount, e.g. 20 mg/m^2, can be considered to be distributed on the surface in several different ways. For conceptual visualization, and for clarification of what can actually be observed in Figure 8k, three example alternatives for the coverage of 20 mg/m^2 are presented in Figure 9. By comparing Figure 8k and Figure 9, the TiO_2 nanocoating with line speed of 300 m/min (50 mg/m^2) can be interpreted to consist mainly of agglomerates of 3-5 primary nanoparticles. Here, the average distance between agglomerates can be estimated to be approximately 100 nm. This distance between nanoparticles is interpreted to be sufficient to obtain superhydrophobic behavior. To support the estimate, the alternative distribution shown in Figure 9c is consistent with the info on the amount of TiO_2. The minimum amount of material to suffice for superhydrophobicity has not been widely discussed in the literature. The recognized references presenting the phenomena of superhydrophobicity and superoleophobicity deal with similar re-entrant structures such as microposts and micro-hoodoo like patterning, but these papers focus merely on micron sized scale [49-51]. Here, we have obviously fabricated structures in the order of 10-100 nm, but still with similar wetting behaviour. It is generally assumed that superhydrophobicity requires a hierarchical, fractal like structure with both micro and nano structures present [XX, YY]. Our result suggests that, at least in the case of our pigment coated paperboard, even a random array with agglomerates of primary nanoparticles, average mutual distances between the agglomerrates in the order of 100 nm would be sufficient for superhydrophobicity.

Based on Figure 3, the threshold value for superhydrophobic behavior can be estimated to be ca. 20 mg/m^2, but since there is relatively large fluctuation in measured data, it may be concluded that 50 mg/m^2 is definitely enough to ensure superhydrophobic behavior. Surface is superhydrophobic also with relatively thick TiO_2 nanoparticle coating. With line speed of 50 m/min, paperboard surface is fully covered with TiO_2 nanoparticles with porous layer of several hundreds of nanometers. This information is necessary for future studies as the thickness of the nanocoating layer can have large variation in coating amount and still the surface is superhydrophobic. This enables easier manufacture of a coating system with several parallel LFS burners.

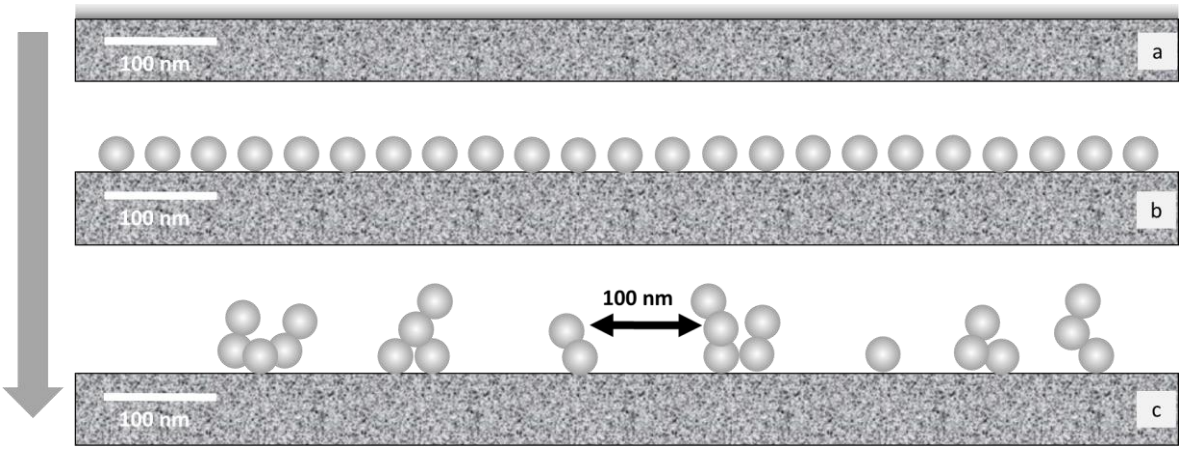

Figure 9: Fixed amount of TiO_2 nanocoating (~ 20 mg/m^2) as three different configurations on the surface of a generic solid substrate: a) solid film (~5 nm), b) evenly distributed single 30 nm nanoparticles and c) agglomerated nanoparticles consisting mainly of 3-5 primary nanoparticles.

The observed minimum amount of nanocoating required for superhydrophobicity gives a tool to optimize the design of the coating. Furthermore, it opens up new possibilities for manufacturing low-cost superhydrophobic surfaces in large quantities. Superhydrophobic paperboard can be used in several applications, e.g. as a packaging material or as a substrate for low cost microfluidistic devices [28].

4 CONCLUSIONS

In this paper, we demonstrated a method for fabricating superhydrophobic surfaces in roll-to-roll process with up to 300 m/min line speeds. With ever-increasing line speeds, it will become relevant which amount of TO_2 would be sufficient to ensure hydrophobicity. Here, nanocoating was performed successfully with all tested line speeds and superhydrophobicity was achieved even if the paperboard surface was only partially covered by TiO_2 nanoparticles, which was verified by SEM imaging. A threshold amount of TiO_2 nanoparticles to provide the superhydrophobicity was approximately 20 mg/m^2. With this coverage, the surface is only partly covered by the nanoparticles, but the gaps between nanoparticles/agglomerates are small enough (~100 nm) for superhydrophobic behavior, the structures resembling the surface patterned re-entrant structures presented previously in the literature, but in micron sized scale. To fabricate superhydrophobic surfaces the coating thickness can have great variations since the superhydrophobicity was observed with all coating amounts exceeding 20 mg/m^2. Superhydrophobicity of the nanocoated surfaces remained and the level of hydrophobicity even increased during the course of 365-day investigation. XPS analysis showed that C/O ratio increased in all samples during the course of 90-day investigation, which indicates accumulation of organic compounds on the surface. This observation is in line with previous studies and explains the increased hydrophobicity in all analyzed samples. Reference paperboard has some micro scale roughness and with addition of TiO_2 nanoparticles, the surface has multi-scale roughness, which enables the superhydrophobic behavior.

While searching for the minimum coating amount of deposited TiO_2 required for superhydrophobicity, the process yield was estimated by the characterization of the total deposited TiO_2 mass. ICP-OES analysis verified the total yield of the LFS nanocoating process (deposited TiO_2 / produced TiO_2) can be with the current setup as high as 43.8 %, depending on the line speed. Total yield and amount of TiO_2 nanoparticles on the LFS treated surface increases significantly from previous studies with optimization of the process parameters, e.g. by tuning the precursor flow rate and decreasing the distance between burner and the substrate (LFS1 vs. LFS2). Minimized amount of nanocoating is economically and environmentally beneficial in most application areas of superhydrophobic surfaces, such as self-cleaning, anti-icing, anti-fogging and anti-biofouling surfaces. Also macro- and microfluidistics as well as oil separation from water and packaging applications would benefit from low-cost manufacturing of superhydrophobic surfaces.

ACKNOWLEDGEMENTS

This work was supported by the Finnish Funding Agency for Innovation (Tekes) under the project “Liquid flame spray nanocoating for flexible roll-to-roll materials” (Nanorata 2). J. Haapanen wishes to thank also Jenny and Antti Wihuri foundation for the financial support. P. Juuti would like to acknowledge TUT graduate school for financial support. Dr. Mari Honkanen (TUT, Laboratory of Materials Science) is acknowledged for the SEM imaging and M.Sc. Pauliina Saloranta (ÅA, Laboratory for Paper Coating and Converting) for the XPS analysis.

REFERENCES

[1] Jin M, Feng X, Xi J, Zhai J, Cho K, Feng L and Jiang L 2005 Super-hydrophobic PDMS surface with ultra-low adhesive force *Macromol. Rapid Commun.* **26** (22) 1805-1809.

[2] Notsu H, Kubo W, Shitanda I and Tatsuma T 2005 Super-hydrophobic/super-hydrophilic patterning of gold surfaces by photocatalytic lithography *J. Mater. Chem.* **15** (15) 1523-1527.

[3] Wu X, Zheng L and Wu D 2005 Fabrication of superhydrophobic surfaces from microstructured ZnO-based surfaces via a wet-chemical route *Langmuir* **21** (7) 2665-2667.

[4] Karapanagiotis I, Grosu D, Aslanidou D and Aifantis K E 2015 Facile method to prepare superhydrophobic and water repellent cellulosic paper *Journal of Nanomaterials* **2015**

[5] Shi F, Wang Z and Zhang X 2005 Combining a layer-by-layer assembling technique with electrochemical deposition of gold aggregates to mimic the legs of water striders *Adv Mater* **17** (8) 1005-1009.

[6] Zhao N, Shi F, Wang Z and Zhang X 2005 Combining layer-by-layer assembly with electrodeposition of silver aggregates for fabricating superhydrophobic surfaces *Langmuir* **21** (10) 4713-4716.

[7] Acatay K, Simsek E, Ow-Yang C and Menceloglu Y Z 2004 Tunable, superhydrophobically stable polymeric surfaces by electrospinning *Angew. Chem. Int. Ed.* **43** (39) 5210-5213.

[8] Liu H, Feng L, Zhai J, Jiang L and Zhu D 2004 Reversible wettability of a chemical vapor deposition prepared ZnO film between superhydrophobicity and superhydrophilicity *Langmuir* **20** (14) 5659-5661.

[9] Karapanagiotis I, Pavlou A, Manoudis P N and Aifantis K E 2014 Water repellent ORMOSIL films for the protection of stone and other materials *Mater Lett* **131** 276-279.

[10] Choi H W, Zhou T, Singh M and Jabbour G E 2015 Recent developments and directions in printed nanomaterials *Nanoscale* **7** (8) 3338-3355.

[11] Dam H F, Andersen T R, Madsen M V, Mortensen T K, Pedersen M F, Nielsen U and Krebs F C 2015 Roll and roll-to-roll process scaling through development of a compact flexo unit for printing of back electrodes *Solar Energy Mater. Solar Cells* **140** 187-192.

[12] Hwang K, Jung Y -, Heo Y -, Scholes F H, Watkins S E, Subbiah J, Jones D J, Kim D - and Vak D 2015 Toward large scale roll-to-roll production of fully printed perovskite solar cells *Adv Mater* **27** (7) 1241-1247.

[13] Luo C, Wang J, Fan X, Zhu Y, Han F, Suo L and Wang C 2015 Roll-to-roll fabrication of organic nanorod electrodes for sodium ion batteries *Nano Energy* **13** 537-545.

[14] Polsen E S, McNerny D Q, Viswanath B, Pattinson S W and John Hart A 2015 High-speed roll-to-roll manufacturing of graphene using a concentric tube CVD reactor *Sci. Rep.* **5**

[15] Kammler H K, Mädler L and Pratsinis S E 2001 Flame synthesis of nanoparticles *Chem. Eng. Technol.* **24** (6) 583-596.

[16] Stark W J and Pratsinis S E 2002 Aerosol flame reactors for manufacture of nanoparticles *Powder Technol* **126** (2) 103-108.

[17] Mueller R, Mädler L and Pratsinis S E 2003 Nanoparticle synthesis at high production rates by flame spray pyrolysis *Chem. Eng. Sci.* **58** (10) 1969-1976.

[18] Loher S, Schneider O D, Maienfisch T, Bokorny S and Stark W J 2008 Micro-organism-triggered release of silver nanoparticles from biodegradable oxide carriers allows preparation of self-sterilizing polymer surfaces *Small* **4** (6) 824-832.

[19] Blattmann C O, Sotiriou G A and Pratsinis S E 2015 Rapid synthesis of flexible conductive polymer nanocomposite films *Nanotechnology* **26** (12)

[20] Rudin T, Tsougeni K, Gogolides E and Pratsinis S E 2012 Flame aerosol deposition of TiO 2 nanoparticle films on polymers and polymeric microfluidic devices for on-chip phosphopeptide enrichment *Microelectron Eng* **97** 341-344.

[21] Mädler L, 2004 Liquid-fed aerosol reactors for one-step synthesis of nano-structured particles *KONA Powder Part. J.* **22** (March) 107-120.

[22] Teoh W Y, Amal R and Mädler L 2010 Flame spray pyrolysis: An enabling technology for nanoparticles design and fabrication *Nanoscale* **2** (8) 1324-1347.

[23] Mäkelä J M, Haapanen J, Harra J, Juuti P and Kujanpää S 2017 Liquid flame spray—a hydrogen-oxygen flame based method for nanoparticle synthesis and functional nanocoatings *KONA Powder Part. J.* **2017** (34) 141-154.

[24] Teisala H, Tuominen M, Stepien M, Haapanen J, Mäkelä J M, Saarinen J J, Toivakka M and Kuusipalo J 2013 Wettability conversion on the liquid flame spray generated superhydrophobic TiO2 nanoparticle coating on paper and board by photocatalytic decomposition of spontaneously accumulated carbonaceous overlayer *Cellulose* **20** (1) 391-408.

[25] Teisala H, Tuominen M, Haapanen J, Aromaa M, Stepien M, Mäkelä J M, Saarinen J J, Toivakka M and Kuusipalo J 2014 Review on liquid flame spray in paper converting: Multifunctional superhydrophobic nanoparticle coatings *Nord Pulp Pap Res J* **29** (4) 747-759.

[26] Stepien M, Saarinen J J, Teisala H, Tuominen M, Aromaa M, Kuusipalo J, Mäkelä J M and Toivakka M 2011 Adjustable wettability of paperboard by liquid flame spray nanoparticle deposition *Appl. Surf. Sci.* **257** (6) 1911-1917.

[27] Mäkelä J M, Aromaa M, Teisala H, Tuominen M, Stepien M, Saarinen J J, Toivakka M and Kuusipalo J 2011 Nanoparticle deposition from liquid flame spray onto moving roll-to-roll paperboard material *Aerosol. Sci. Technol.* **45** (7) 817-827.

[28] Songok J, Tuominen M, Teisala H, Haapanen J, Mäkelä J, Kuusipalo J and Toivakka M 2014 Paper-based micro fluidics: Fabrication technique and dynamics of capillary-driven surface flow *ACS Appl. Mater. Interfaces* **6** (22) 20060-20066.

[29] Brobbey K J, Haapanen J, Gunell M, Mäkelä J M, Eerola E, Toivakka M and Saarinen J J 2017 One-step flame synthesis of silver nanoparticles for roll-to-roll production of antibacterial paper *Appl. Surf. Sci.* **420** 558-565.

[30] Haapanen J, Aromaa M, Teisala H, Tuominen M, Stepien M, Saarinen J J, Heikkilä M, Toivakka M, Kuusipalo J and Mäkelä J M 2015 Binary TiO2/SiO2 nanoparticle coating for controlling the wetting properties of paperboard *Mater. Chem. Phys.* **149** 230-237.

[31] Tuominen M, Teisala H, Aromaa M, Stepien M, Mäkelä J M, Saarinen J J, Toivakka M and Kuusipalo J 2014 Creation of superhydrophilic surfaces of paper and board *J. Adhes. Sci. Technol.* **28** (8-9) 864-879.

[32] Tikkanen J, Gross K A, Berndt C C, Pitkänen V, Keskinen J, Raghu S, Rajala M and Karthikeyan J 1997 Characteristics of the liquid flame spray process *Surf. Coat. Technol.* **90** (3) 210-216.

[33] Gross K A, Tikkanen J, Keskinen J, Pitkänen V, Eerola M, Siikamaki R and Rajala M 1999 Liquid flame spraying for glass coloring *J. Therm. Spray Technol.* **8** (4) 583-589.

[34] Ejenstam L, Tuominen M, Haapanen J, Mäkelä J M, Pan J, Swerin A and Claesson P M 2015 Long-term corrosion protection by a thin nano-composite coating *Appl. Surf. Sci.* **357** 2333-2342.

[35] Moghaddam M S, Heydari G, Tuominen M, Fielden M, Haapanen J, Mäkelä J M, Wålinder M E P, Claesson P M and Swerin A 2016 Hydrophobisation of wood surfaces by combining liquid flame spray (LFS) and plasma treatment: Dynamic wetting properties *Holzforschung* **70** (6) 527-537.

[36] Saarinen J J, Valtakari D, Haapanen J, Salminen T, Mäkelä J M and Uozumi J 2014 Surface-enhanced Raman scattering active substrates by liquid flame spray deposited and inkjet printed silver nanoparticles *Opt. Rev.* **21** (3) 339-344.

[37] Juuti P, Haapanen J, Stenroos C, Niemelä-Anttonen H, Harra J, Koivuluoto H, Teisala H, Lahti J, Tuominen M, Kuusipalo J, Vuoristo P and Mäkelä J M 2017 Achieving a slippery, liquid-infused porous surface with anti-icing properties by direct deposition of flame synthesized aerosol nanoparticles on a thermally fragile substrate *Appl. Phys. Lett.* **110** (16)

[38] Mäkelä J M, Aromaa M, Rostedt A, Krinke T J, Janka K, Marjamäki M and Keskinen J 2009 Liquid flame spray for generating metal and metal oxide nanoparticle test aerosol *Hum. Exp. Toxicol.* **28** (6-7) 421-431.

[39] Tuominen M, Teisala H, Haapanen J, Mäkelä J M, Honkanen M, Vippola M, Bardage S, Wålinder M E P and Swerin A 2016 Superamphiphobic overhang structured coating on a biobased material *Appl. Surf. Sci.* **389** 135-143.

[40] Teisala H, Geyer F, Haapanen J, Juuti P, Mäkelä J M, Vollmer D and Butt H - 2018 Ultrafast Processing of Hierarchical Nanotexture for a Transparent Superamphiphobic Coating with Extremely Low Roll-Off Angle and High Impalement Pressure *Adv Mater* **30** (14)

[41] Stepien M, Saarinen J J, Teisala H, Tuominen M, Aromaa M, Haapanen J, Kuusipalo J, Mäkelä J M and Toivakka M 2013 ToF-SIMS analysis of UV-switchable TiO2-nanoparticle-coated paper surface *Langmuir* **29** (11) 3780-3790.

[42] Stepien M, Saarinen J J, Teisala H, Tuominen M, Aromaa M, Kuusipalo J, Mäkelä J M and Toivakka M 2012 Surface chemical analysis of photocatalytic wettability conversion of TiO 2 nanoparticle coating *Surf. Coat. Technol.* **208** 73-79.

[43] Stepien M, Saarinen J J, Teisala H, Tuominen M, Haapanen J, Mäkelä J M, Kuusipalo J and Toivakka M 2013 Compressibility of porous TiO2 nanoparticle coating on paperboard *Nanoscale Res. Lett.* **8** (1) 1-6.

[44] Stepien M, Chinga-Carrasco G, Saarinen J J, Teisala H, Tuominen M, Aromaa M, Haapanen J, Kuusipalo J, Mäkelä J M and Toivakka M 2013 Wear resistance of nanoparticle coatings on paperboard *Wear* **307** (1-2) 112-118.

[45] Kanta A, Sedev R and Ralston J 2005 Thermally- and photoinduced changes in the water wettability of low-surface-area silica and titania, *Langmuir* **21** 2400-2407.

[46] Takeda S, Fukawa M, Hayashi Y and Matsumoto K 1999 Surface OH group governing adsorption properties of metal oxide films *Thin Solid Films* **339** (1-2) 220-224.

[47] Castillo J L, Martin S, Rodriguez-Perez D, Perea A and Garcia-Ybarra P L 2014 Morphology and nanostructure of granular materials built from nanoparticles *KONA Powder Part. J.* **31** (1) 214-233.

[48] Mädler L, Lall A A and Friedlander S K 2006 One-step aerosol synthesis of nanoparticle agglomerate films: Simulation of film porosity and thickness *Nanotechnology* **17** (19) 4783-4795.

[49] Tuteja A, Choi W, Ma M, Mabry J M, Mazzella S A, Rutledge G C, McKinley G H and Cohen R E 2007 Designing superoleophobic surfaces *Science* **318** (5856) 1618-1622.

[50] Liu T and Kim C - 2014 Turning a surface superrepellent even to completely wetting liquids *Science* **346** (6213) 1096-1100.

[51] Choi H -, Choo S, Shin J -, Kim K - and Lee H 2013 Fabrication of superhydrophobic and oleophobic surfaces with overhang structure by reverse nanoimprint lithography *J. Phys. Chem. C* **117** (46) 24354-24359.